

# Contribution To Environmental Protection By Reducing Pollutants Emissions During Municipal Solid Wastes Incineration

K. N'wuitcha, K. Palm, S.W. Igo, K. Atchonouglo, A. Ndiho, I. Ouedraogo, M. Banna, B. Zeghmati

**Abstract:** The purpose of this study is to contribute to environmental protection by reducing pollutants emission during municipal solid waste incineration. This paper presents the mathematical model for predicting the thermal treatment of the fumes produced by the combustion of municipal solid waste, in turbulent regime, before discharge into the atmosphere. Forced turbulent equations associated to radiative transfer equation are proposed and solved. The standard k-epsilon model was used for the modeling of the turbulence phenomena in the incinerator. The turbulence-chemistry interaction is depicted by Eddy-Dissipation model. Discrete ordinate method is used for the modeling of the radiative heat transfer. The equations are solved using an implicit scheme based on the finite volume method. The results show that the thermal treatment process is more efficient with low Reynolds number. The radiative transfer intensifies convective transfers and increases the temperature of the smoke. This transfer mode enhances the thermo destruction process effectiveness.

**Index Terms:** Incineration, modeling, municipal solid wastes, pollutants, thermal treatment, turbulent regime, radiative transfer.

## 1 INTRODUCTION

INCINERATION is a method of waste destruction in a furnace by controlled burning at high temperatures [1]. Incineration and other high temperature waste treatment systems are described as "thermal treatment". Incineration of waste materials converts the waste into ash, flue gas, and heat. The ash is mostly formed by the inorganic constituents of the waste, and may take the form of solid lumps or particulates carried by the flue gas.

In recent years, incineration has frequently been preferred to other waste treatment or disposal alternatives due to advantages such as [2-4]: the volume and mass of municipal solid waste is reduced to a fraction of its original size (by 85-90 % volume); the waste reduction is immediate and not dependent on long biological break-down reaction times; incineration facilities can be constructed closer to the municipal solid waste sources or collection points, reducing transportation costs; using heat recovery technology, the cost of the operation can be offset by energy sales; air discharges can be controlled to meet environmental legislative limit values. However, incineration has a number of outputs such as the ash and the emission to the atmosphere of flue gas. The flue gases may contain significant amounts of particulate matter, heavy metals, dioxins, furans, sulfur dioxide, and hydrochloric acid [5]. The public health impact associated with emissions from municipal solid waste has become and continues to be a major subject of concern due to the following reasons [4]: some materials should not be incinerated because they are more valuable for recycling, they are non-combustible or their by-products may give rise to harmful emissions; poor operating practices and the presence of chlorine in the municipal solid waste may lead to emissions containing highly toxic dioxins and furans; the control of metal emissions may be difficult for inorganic wastes containing heavy metals, such as arsenic, cadmium, chromium, copper, lead, mercury, nickel, etc.; incinerators require a high capital costs and trained operators leading to moderately high operating costs; supplementary fuels are required to achieve the necessary high combustion temperatures. Taking above mentioned aspects into consideration the flue gases must be cleaned of gaseous and particulate pollutants before they are dispersed into the atmosphere. The quantity of pollutants in the flue gas from incineration plants may or may not be reduced by several processes, depending on the plant. Particulate is collected by particle filtration, most often electrostatic precipitators and/or baghouse filters. The latter are generally very efficient for collecting fine particles [6]. Acid gas scrubbers are used to remove hydrochloric acid, nitric acid, hydrofluoric acid, mercury, lead and other heavy metals [7]. The efficiency of removal will depend on the specific equipment, the chemical composition of the waste, the design of the plant, the chemistry of reagents, and the ability of

- K. N'wuitcha, GPTE-LES, University of Lome, PO Box 1515, Lome, Togo. E-mail: [nwuitchakokou@yahoo.fr](mailto:nwuitchakokou@yahoo.fr)
- K. Palm, IRSAT/CNRST-Department of Energy, 03 PO Box 7047, Ouagadougou 03, Burkina Faso. E-mail: [palm\\_kalifa@hotmail.com](mailto:palm_kalifa@hotmail.com)
- S. W. Igo, IRSAT/CNRST-Department of Energy, 03 PO Box 7047, Ouagadougou 03, Burkina-Faso. E-mail: [sergesigo@yahoo.fr](mailto:sergesigo@yahoo.fr)
- K. Atchonouglo, GPTE-LES, University of Lome, PO Box 1515, Lome, Togo. E-mail: [kossi.atchonouglo@gmail.com](mailto:kossi.atchonouglo@gmail.com)
- Ndiho, GPTE-LES, University of Lome, PO Box 1515, Lome, Togo. E-mail: [ndaimable2000@yahoo.fr](mailto:ndaimable2000@yahoo.fr)
- Ouédraogo, Laboratoire de Chimie organique et Physique appliquée UFR\SEA Université de Ouagadougou, 03 BP 7021 Ouagadougou 03, Burkina Faso E-mail: [issaka.ouedraogo@univ-ouaga.bf](mailto:issaka.ouedraogo@univ-ouaga.bf)
- M. Banna, GPTE-LES, University of Lome, PO Box 1515, Lome, Togo. E-mail: [maqbanna@yahoo.fr](mailto:maqbanna@yahoo.fr)
- Zeghmati, LA.M.P.S-GME, University of Perpignan Via Domitia, 52 Avenue Paul Alduy, 66860 Perpignan Cedex, France, E-mail: [zeghmati@univ-perp.fr](mailto:zeghmati@univ-perp.fr)

engineers to optimize these conditions, which may conflict for different pollutants. Sulfur dioxide may also be removed by dry desulfurisation by injection limestone slurry into the flue gas before the particle filtration. NO<sub>x</sub> is either reduced by catalytic reduction with ammonia in a catalytic converter (selective catalytic reduction, SCR) [8,9] or by a high temperature reaction with ammonia in the furnace (selective non-catalytic reduction, SNCR) [10,11]. Heavy metals are often adsorbed on injected active carbon powder, which is collected by the particle filtration. Several processes of treatment and energy valorization of waste incineration effluents were also proposed [12-14], but the incineration remains at present the most promising technique of depollution [12]. Halouani and Farhat [15] studied the depollution of atmospheric emissions of wood pyrolysis furnaces. Their results show that the incineration, at about 1000°C of wood carbonization smokes allow the destruction of 99% of the mass of pollutants except CO<sub>2</sub> and the reduction of polluting gas emission. In the present work a detailed investigation has been carried out on the modeling of the thermal treatment of the fumes produced by the combustion of municipal solid waste, in turbulent regime. This study aimed to reduce the quantity of the pollutant components of smoke and to analyze the effect of Reynolds number, radiation and the relative positions of inlet and outlet port on the efficiency of thermo destruction process.

## 2 PHYSICAL AND MATHEMATICAL MODEL

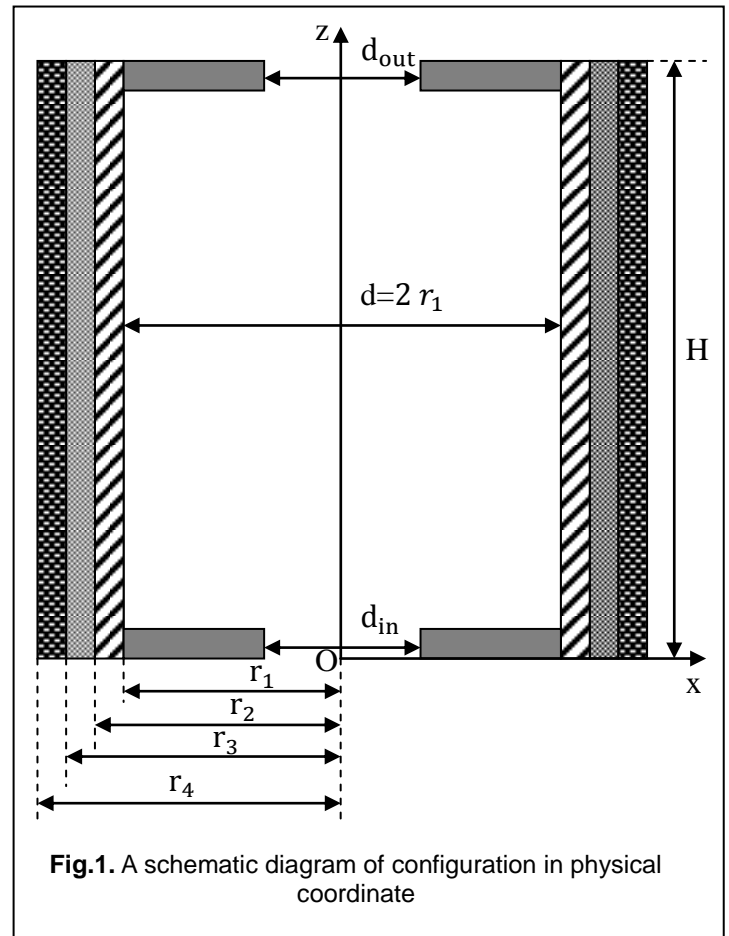
### 2.1. Incinerator configuration and assumptions

The case studied is a typical chamber of gaseous combustion, namely a cylindrical enclosure of 0.5 m radius and 1 m height [16]. The walls of the incinerator are made of refractory bricks, insulated with glass wool layer imprisoned in a metallic sheet. The smokes from household wastes combustion enters in the incinerator through a lower port ( $d_{in}=0.20$  m). After the thermo-destruction process the gas mixture is rejected into atmosphere through a port ( $d_{out}=0.20$  m) located in the middle of the top wall. The overall geometry of the incinerator is illustrated in Fig. 1. The following assumptions are made in formulating the mathematical model for the thermo destruction process of the fumes produced by municipal waste combustion.

- the viscous dissipation is neglected;
- the Dufour and Soret effects are neglected;
- the furnace walls are gray, diffusively emitting and reflecting;
- the fumes are composed of CH<sub>4</sub>, C<sub>2</sub>H<sub>4</sub>, CO, and H<sub>2</sub>
- the smokes are assimilated to an ideal gas and supposed to be a grey and diffusing medium the flow is considered to be incompressible, turbulent and two-dimensional.

### 2.2. Mathematical model

The governing equations for mass, momentum, species and



energy conservation in the fumes are given in conservative differential form in cylindrical coordinates ( $r, z$ ), in terms of variables such as velocities ( $u, v$ ), pressure ( $P$ ), density ( $\rho$ ), masse fraction of species "i" ( $Y_i$ ), temperature ( $T$ ). The turbulence kinetic energy ( $k$ ) and the dissipation of turbulent kinetic energy ( $\epsilon$ ) are calculated with the  $k - \epsilon$  model [17].

#### Continuity equation

The mass continuity of the reacting flow may be written as

$$\partial \rho / \partial t + \partial(\rho u) / \partial z + \partial(\rho r v) / r \partial r = 0 \quad (1)$$

#### Momentum equation

The momentum equation for turbulent reacting flow may be written as:

$$\begin{aligned} \partial(\rho u) / \partial t + \partial(\rho u u) / \partial z + \partial(\rho r v u) / (r \partial r) \\ = 2[\partial(\mu_e \partial u / \partial z) / \partial z + \partial(r \mu_e \partial u / \partial r) / (r \partial r)] \\ - \partial P / \partial z + \rho g \end{aligned} \quad (2)$$

$$\begin{aligned} \partial(\rho v) / \partial t + \partial(\rho u v) / \partial z + \partial(\rho r v v) / (r \partial r) \\ = 2[\partial(\mu_e \partial v / \partial z) / \partial z + \partial(r \mu_e \partial v / \partial r) / (r \partial r)] \\ - \partial P / \partial r - 2\mu_e v / r^2 \end{aligned} \quad (3)$$

in which  $\mu_e$  is the effective viscosity defined by  $\mu_e = \mu + \mu_t$ , where  $\mu_t$  is the turbulent viscosity, and  $\mu$  the dynamic fluid viscosity. The turbulent viscosity  $\mu_t$  has the following relation with turbulent kinetic energy  $k$  and its dissipation  $\epsilon$

$$\mu_t = C_\mu k^2 / \varepsilon \quad (4)$$

$C_\mu$ , denoting an experimental constant.

### Energy equation

The energy equation for the reacting flow is

$$\begin{aligned} \partial(\rho T) / \partial t + \partial(\rho u T) / \partial z + \partial(\rho r v T) / (r \partial r) \\ = \partial[(\lambda / C_p + \mu_t / Pr_t)(\partial T / \partial z)] / \partial z \\ + \partial[r(\lambda / C_p + \mu_t / Pr_t)(\partial T / \partial r)] / (r \partial r) + S_h \end{aligned} \quad (5)$$

Where:

- $S_h$  denotes the volumetric heat quantity released by the chemical reactions and the radiative transfer,
- $\lambda$  is the thermal conductivity
- $C_p$  is the specific heat at constant pressure.
- $Pr_t$  is the turbulent Prandtl number

### Mass transfer equation

The species equation for all reacting species is

$$\begin{aligned} \partial(\rho Y_i) / \partial t + \partial(\rho u Y_i) / \partial z + \partial(\rho r v Y_i) / (r \partial r) \\ = \partial[(\rho D_i + \mu_t / Sc_t) \partial Y_i / \partial z] / \partial z \\ + \partial[r(\rho D_i + \mu_t / Sc_t) (\partial Y_i / \partial r)] / (r \partial r) + R_i, \end{aligned} \quad (6)$$

$R_i$  denoting the volumetric mass rate of species  $i$  ( $CH_4$ ,  $C_2H_4$ ,  $CO$ ,  $H_2$ ,  $O_2$ ,  $CO_2$ ,  $H_2O$ )

The turbulent kinetic energy ( $k$ ) and its dissipation rate ( $\varepsilon$ ) appearing in equation (4) can be obtained by solving the  $k$ -equation and  $\varepsilon$ -equation, which are put in the following way:

### $k$ -equation

$$\begin{aligned} \partial(\rho k) / \partial t + \partial(\rho u k) / \partial z + \partial(\rho r v k) / (r \partial r) \\ = \partial[(\mu + \mu_t / \sigma_k) (\partial k / \partial z)] / \partial z \\ + \partial[r(\mu + \mu_t / \sigma_k) (\partial k / \partial r)] / (r \partial r) + G_k - \rho \varepsilon \end{aligned} \quad (7)$$

### $\varepsilon$ -equation

$$\begin{aligned} \partial(\rho \varepsilon) / \partial t + \partial(\rho u \varepsilon) / \partial z + \partial(\rho r v \varepsilon) / (r \partial r) \\ = \partial[(\mu + \mu_t / \sigma_\varepsilon) (\partial \varepsilon / \partial z)] / \partial z \\ + \partial[r(\mu + \mu_t / \sigma_\varepsilon) (\partial \varepsilon / \partial r)] / (r \partial r) \\ + \varepsilon (C_{\varepsilon 1} G_k - C_{\varepsilon 2} \rho \varepsilon) / k \end{aligned} \quad (8)$$

The model empirical constants appearing in the above equations are assigned the values given in Table 1 [17].

**TABLE 1**

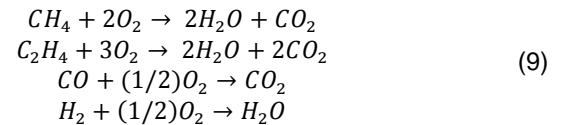
THE VALUES OF THE EMPIRICAL CONSTANTS IN THE HIGH-REYNOLDS-NUMBER FORM OF  $k - \varepsilon$  MODEL OF TURBULENCE

$C_\mu$	$C_{\varepsilon 1}$	$C_{\varepsilon 2}$	$\sigma_k$	$\sigma_\varepsilon$
0.09	1.55	2.0	1.0	1.3

### Combustion model

The fluid flow and chemical reaction must be defined, for the combustion of the components of the smoke generated by household wastes incineration. The smoke is a mixture of hydrocarbons such as methane ( $CH_4$ ) and ethylene ( $C_2H_4$ ),

hydrogen ( $H_2$ ) and monoxide of carbon ( $CO$ ). In the present work, the following global single-step reactions for smoke components combustion in air are used.



Reaction rate in turbulent flow is calculated by the eddy-dissipation model [18] which is given as:

$$R_{i,r} = v'_{i,r} M_i A \rho (\varepsilon / k) \min(Y_R / v'_{R,r} M_R) \quad (10)$$

Or

$$R_{i,r} = v'_{i,r} M_i B \rho (\varepsilon / k) (\sum Y_P / \sum v'_{j,r} M_j) \quad (11)$$

Where:

$Y_R, Y_P$  are mass fractions of reactants R and products P respectively;  $A$  et  $B$ : empirical constants ( $A = 4.0; B = 0.5$ ).  $M_i$ : molecular weight of specie  $i$

### Radiation modelling

The radiative transfer equation (RTE) for absorbing, emitting, and scattering medium at position  $\vec{r}$  in the direction  $\vec{S}$  is given as [19]

$$\begin{aligned} \partial(\xi I) / \partial z + \partial(\gamma r I) / (r \partial r) - \partial(\eta I) / (r \partial \phi) = \\ -(k_a + \sigma_s) I + k_a I_b + (\sigma_s / 4\pi) \int_{\Omega'} I \Phi(\vec{S}', \vec{S}) d\Omega \end{aligned} \quad (12)$$

Where

$I$  radiative intensity

$I_b$  blackbody radiative intensity

$\xi, \gamma, \eta$  are direction cosines,

$\vec{S}, \vec{S}'$  are direction vector and scattering direction vector,

$k_a, \sigma_s$  are absorption coefficient and scattering coefficient,

$\Phi$  is phase function,

$\phi$  angular azimuthal angle

$\Omega, \Omega'$  solid angles.

### Initial and boundaries conditions

The initial and boundary conditions for the problem are

$t \leq t_0$ :

$$0 \leq r \leq d/2 \text{ and } 0 \leq z \leq H$$

$$u = v = 0, Y_k = Y_{kin}, T = T_{in}, k = k_{in}, \varepsilon = \varepsilon_{in} \quad (13)$$

$t \geq t_0$ :

$$0 \leq r \leq d_{in}/2 \text{ and } z = 0$$

$$\begin{aligned} u = u_{in}, v = 0, Y_k = Y_{kin}, T = T_{in}, I = \varepsilon_g \sigma T_{in}^4 / \pi \\ k = 0.005 U_{in}^2; \varepsilon = 2 C_\mu k^{3/2} / (0.03 d_{in}), \end{aligned} \quad (14)$$

$$0 \leq r \leq d_{out}/2 \text{ and } z = H$$

$$\partial u / \partial z = 0, \partial v / \partial z = 0, \partial Y_i / \partial z = 0, \partial T / \partial z = 0$$

$$\partial k / \partial z = 0, \partial \varepsilon / \partial z = 0, I = \varepsilon_g \sigma T_{out}^4 / \pi \quad (15)$$

$$r = d/2 \text{ and } 0 \leq z \leq H$$

$$u = v = 0, \partial Y_i / \partial r = 0, k = 0$$

$$\varepsilon = 2(\mu/\rho)(\partial k^{1/2} / \partial r)^2 \tag{16}$$

$$2\pi r_1 H \lambda \partial T / \partial r = (T_{w_{in}} - T_{w_{out}}) / R_t = 2\pi r_1 H h_{air} (T_{w_{out}} - T_{amb})$$

with

$$R_t = (\sum_{l=1}^3 (1/3) \log(r_{l+1}/r_l)) / 2\pi H$$

where  $\lambda_l$  is the layer  $l$  conductivity,  $r_l$  and  $r_{l+1}$  are two consecutive radius of the cylindrical surfaces delimiting the layer  $l$ .

$$d_{in}/2 \leq r \leq d/2 \text{ and } z = 0$$

$$u = v = 0, \partial Y_i / \partial z = 0, \partial T / \partial z = 0 \quad k = 0$$

$$\varepsilon = 2(\mu/\rho)(\partial k^{1/2} / \partial z)^2 \tag{17}$$

$$d_{out}/2 \leq r \leq d/2 \text{ and } z = H$$

$$u = v = 0, \partial Y_i / \partial z = 0, \partial T / \partial z = 0 \quad k = 0$$

$$\varepsilon = 2(\mu/\rho)(\partial k^{1/2} / \partial z)^2 \tag{18}$$

$$r = 0 \text{ and } 0 \leq z \leq H$$

$$\partial u / \partial r = 0, \partial v / \partial r = 0, \partial Y_i / \partial r = 0, \partial T / \partial r = 0$$

$$\partial k / \partial r = 0, \partial \varepsilon / \partial r = 0, \partial I / \partial r = 0 \tag{19}$$

On walls:

$$I_w = \varepsilon_w (\sigma T_w^4 / \pi + ((1 - \varepsilon_w) / \pi)) \int_{\vec{n}_w \cdot \vec{\Omega} > 0} I_w |\vec{n}_w \cdot \vec{\Omega}| d\Omega' \tag{20}$$

where  $\varepsilon_w$  is the wall emissivity and  $\vec{n}_w$  represents the unit normal vector on the wall.

### 3. Numerical procedure

A finite volume method is used for the discretization of the governing equations (1) - (8). The one for the RTE (11) is the discrete coordinate method. The resulting algebraic equations are solved using Gauss Seidel iterative method and under-relaxation factors (0.6 for  $u$  and  $v$ ; 0.8 for the others parameters). Convergence of this iterative procedure is declared when the relative variations of any dependent variable is less than  $10^{-4}$  and the mass residual falls below  $10^{-6}$  at all the grid points. In order to ensure the grid-independence solution, computations were performed using different size grids: (51x51), (61x61), (81x81), (101x101), (131x131) for various Reynolds number. An increase of the grid size from (51x51) to (61x61) leads to a discrepancy of 0.19%, 0.009%, 0.045% and 1.159% respectively for the maximum local Nusselt number, the stream function, the axial and radial velocity component (Table 2). Thus, we choose the grid (51x51); it corresponds to the following grid step:  $\Delta r = 0.01$ ;  $\Delta z = 0.02$ .

**TABLE 2**  
EFFECT OF GRID SIZE FOR RE=5000

Grids	Nu <sub>z,max</sub> at r=R	U <sub>max</sub> at z=0,5	V <sub>max</sub> at z=0,5	ψ <sub>max</sub>	μ <sub>t,max</sub>
51x51	55.8261	0.413744	0.0181427	0.04853	7.5629x10 <sup>-4</sup>
61x61	55.8284	0.4142	0.0176445	0.04862	7.5788x10 <sup>-4</sup>
81x81	75.9318	0.413267	0.0186186	0.04872	7.6482x10 <sup>-4</sup>
101x101	94.0672	0.412576	0.0166763	0.04896	7.8162x10 <sup>-4</sup>
131x131	98.0465	0.407878	0.0118862	0.04953	8.2979x10 <sup>-4</sup>

The accuracy of the numerical model was checked by comparing the results from the present study with those reported in [20]. As shown in Fig.2 ours results are in good agreement with the experimental velocity and temperatures of [20]. The maximum discrepancy is less than 3.5% for the vertical component velocity and about 4% for the temperature.

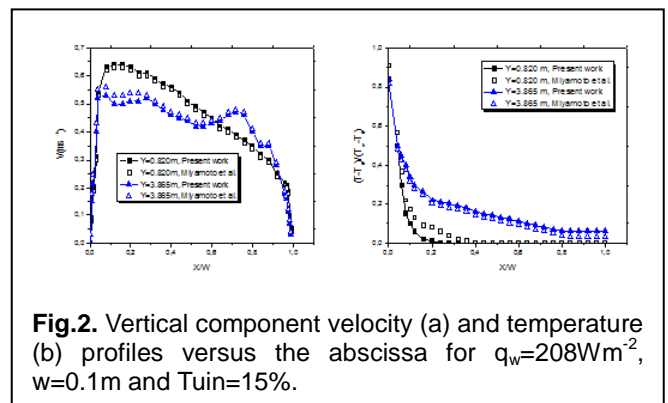


**Fig.2.** Vertical component velocity (a) and temperature (b) profiles versus the abscissa for  $q_w=208Wm^{-2}$ ,  $w=0.1m$  and  $T_{u,in}=15\%$ .

### 4. Results and discussion

A numerical study has been performed through finite volume method to analyze the turbulent combustion of smoke components and its effects on the fluid flow and heat transfer in the incinerator. The effects of Reynolds number and radiation on heat transfer, fluid flow and thermo destruction efficiency are examined. Reynolds number was varied in the range of 5000 to 20000, the aspect ratio  $H/D$  and  $d_{in}/D$ , respectively equal to 1 and 1/5. The emissivity of the incinerator wall is taken equal 0.8. The inlet mass fractions of the smoke produced by the combustion of household wastes are given in Table 3.

**TABLE 3**  
CHEMICAL ANALYSIS OF THE SMOKE AT THE INLET OF THE INCINERATOR

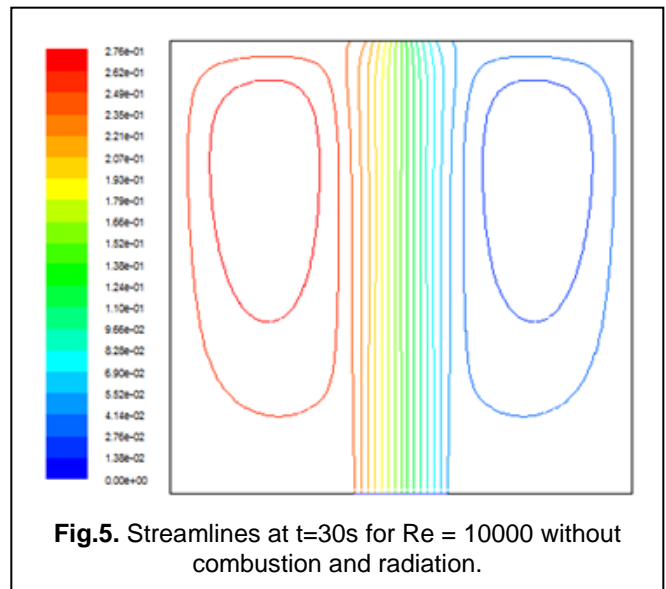
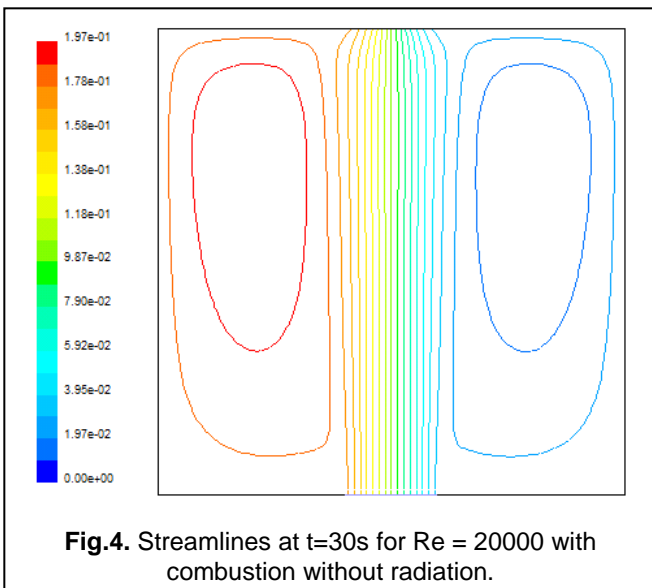
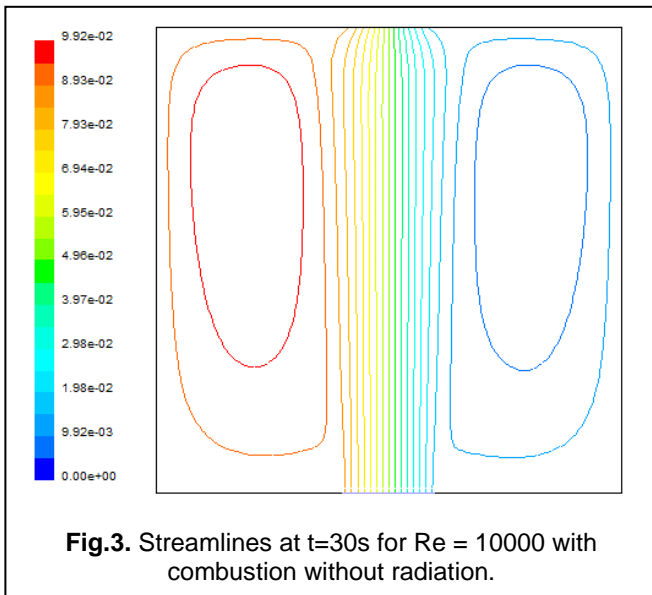
Smoke Components	CH <sub>4</sub>	C <sub>2</sub> H <sub>4</sub>	CO	H <sub>2</sub>	O <sub>2</sub>	N <sub>2</sub>	CO <sub>2</sub>	H <sub>2</sub> O
Mass Fractions(%)	0.38	0.23	1.29	0.03	16.77	67.07	2.55	11.66

#### 4.1 Flow field

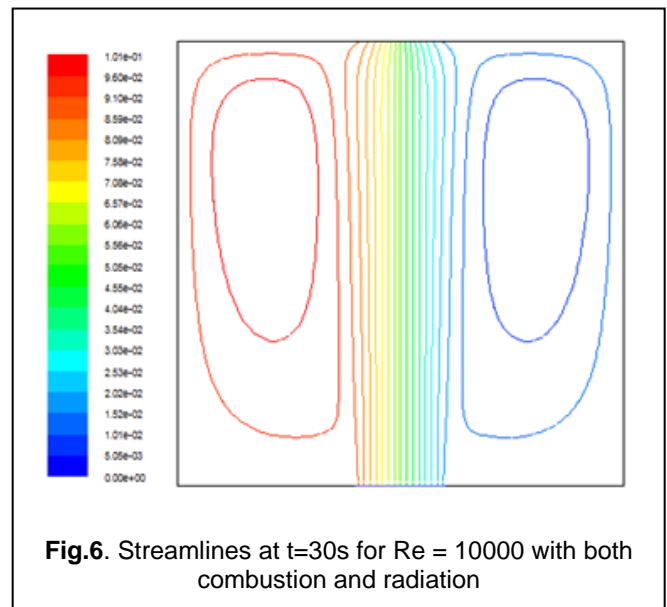
Flow field is simulated using streamlines. The streamlines of the flow for  $Re = 10000$  and  $Re = 20000$  are shown in Fig. 1 and 2 respectively. For the two Reynolds number studied, the flow is symmetric with the centerline of the channel without deflecting into one side. There are two counter-rotating cells located on



both side of the symmetrical vertical axis of the incinerator along which the mean flow is developed between the inlet and outlet ports. The mean flow is characterized by parallel streamlines. The increase of the Reynolds number leads to an increase of the streamlines values without changing the size of the counter-rotating cells. This is mainly because the effect of convection becomes intensive as the Reynolds number increases. Fig.5 shows the flow structure when combustion and radiation are not took into account. A comparison between streamlines values shown in Fig. 3 and those of Fig.5 shows that the heat released by the combustion of smoke components

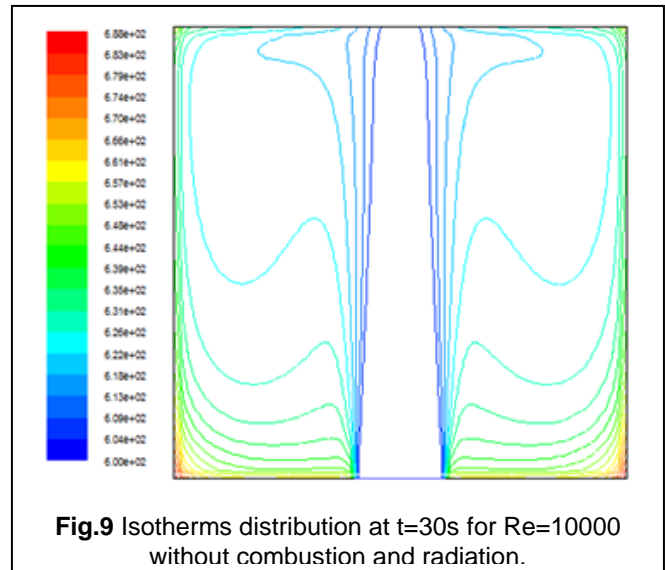
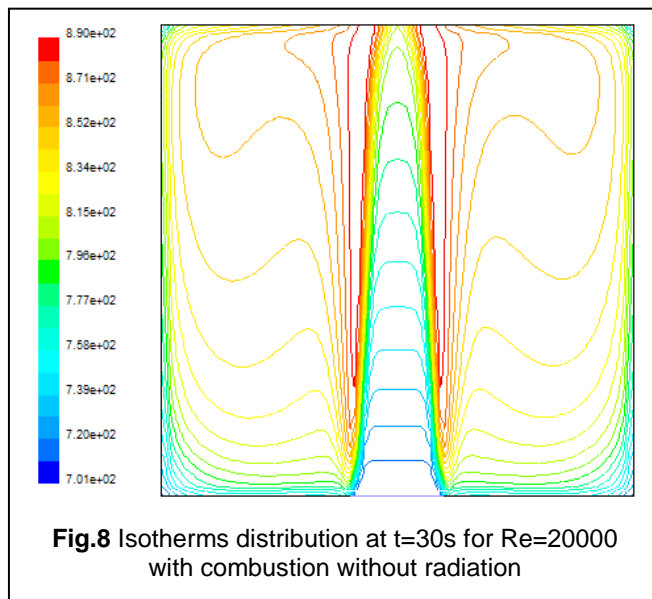
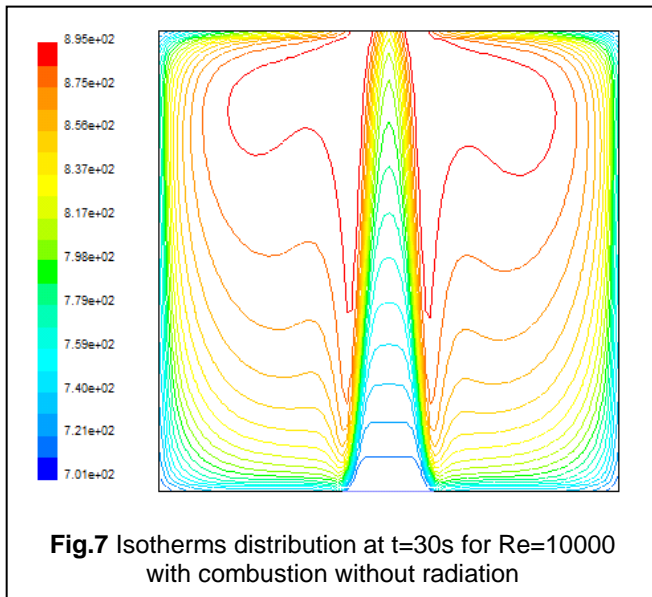


Intensifies transfers but the flow structure is weak altered. The amount of heat released by the combustion process increases the temperature of the flow and the walls of the incinerator. Consequently the natural convection flow generated by the temperature and mass fraction gradient combines with the turbulent forced convection leads to a weak modification of the flow structure. The flow pattern is also examined to investigate the effect of radiative transfer on the flow structure. It can be observed that the radiative heat transfer has no effect on the flow structure (Fig. 3 and 6). However the radiative heat transfer increases the streamline values because the transfer mode increases the flow temperature. The maximum value of the streamline is equal to  $9.92e^{-02} \text{ m}^2\text{s}^{-1}$  for the reactive flow without the radiative heat transfer and to  $1.01e^{-01} \text{ m}^2\text{s}^{-1}$  when the radiative heat transfer is taken into account.

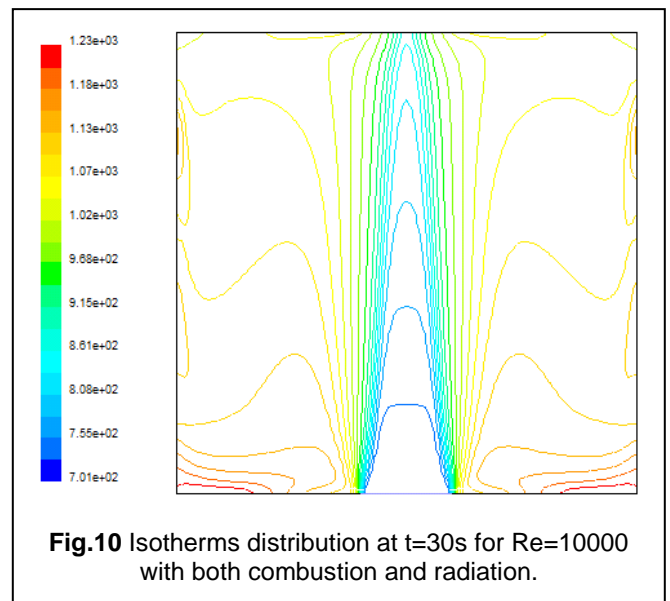


#### 4.2 Temperature fields

The temperature fields are displayed in Fig. 7 and 8 for two different Reynolds number ( $Re = 10000$  and  $Re = 20000$ ) when combustion is taken into account without radiation. It can be noted that as streamlines, isotherms are located on both side of the symmetrical vertical axis of the incinerator and are symmetric with this axis. They start at the inlet and then are warped by the flow along the symmetrical vertical axis and the heat loss through the vertical walls. The effect of Reynolds number on isotherms is illustrated by Fig.7 and 8. It can be seen that the isotherms fields are weakly modified when the Reynolds number increases but the isotherms values decreases with the increasing Reynolds number because of the intensification of convective transfer which reduces the residence time of smoke pollutants in the incinerator.



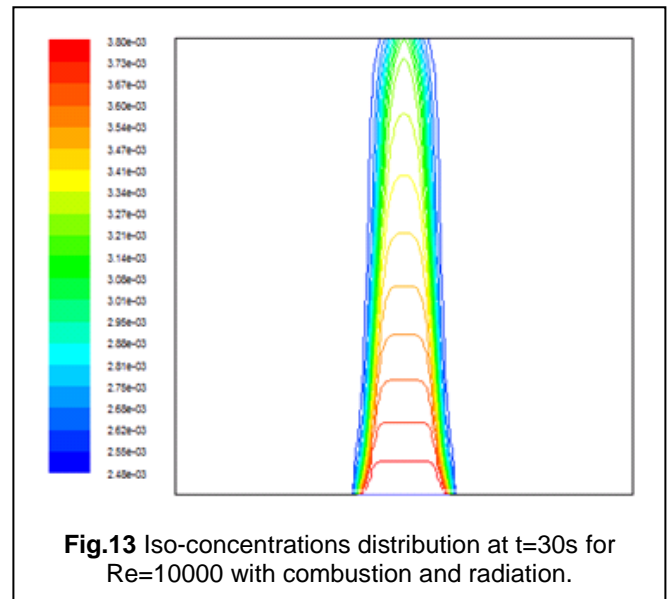
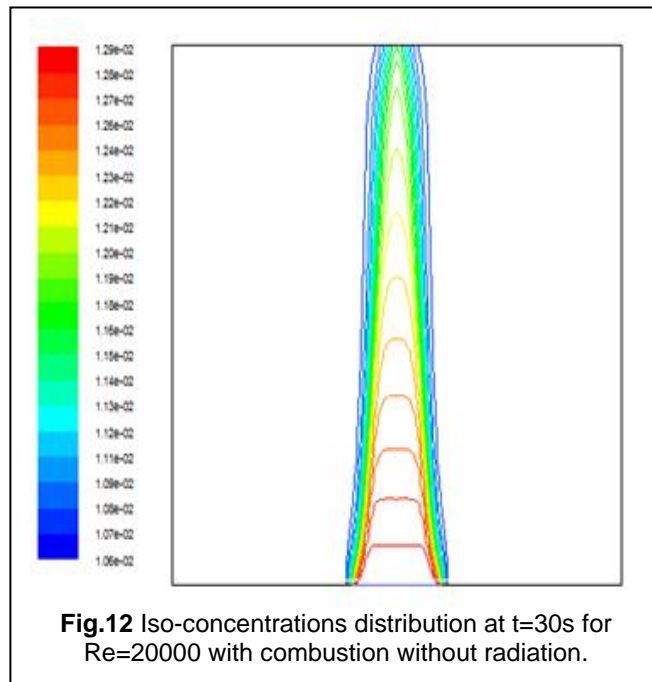
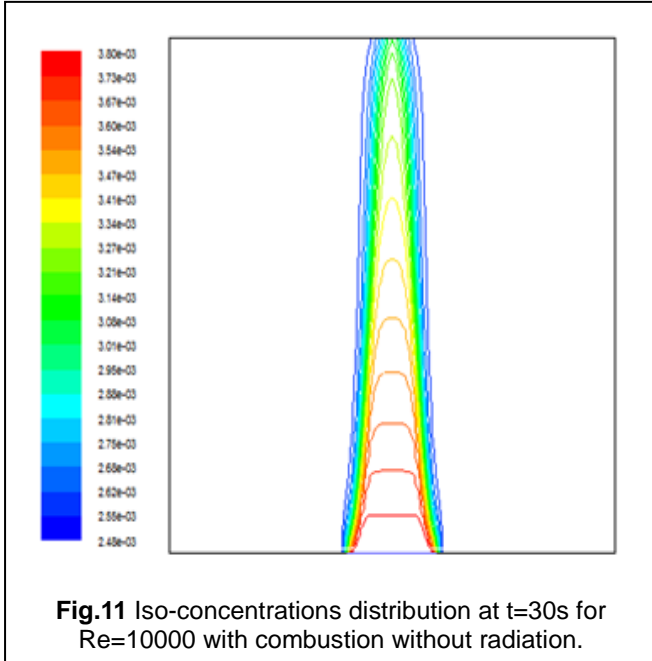
As for the flow structure, the heat quantity produced by the smoke pollutants combustion increases the isotherms patterns and the temperature values (Figs 7 and 9). We reported above that the radiative heat transfer increases the convection intensity. Consequently, though the isotherms fields are weakly modified, the temperature increases notably in the zones located on both side of the incinerator symmetrical vertical axis (Fig.7 and 10). The maximum value which is equal to 895 K (Fig.7), when taking into account combustion and neglecting radiation, increases up to 1230 K when the radiative heat transfer is taken into account in the combustion of smoke pollutants (Fig.10).



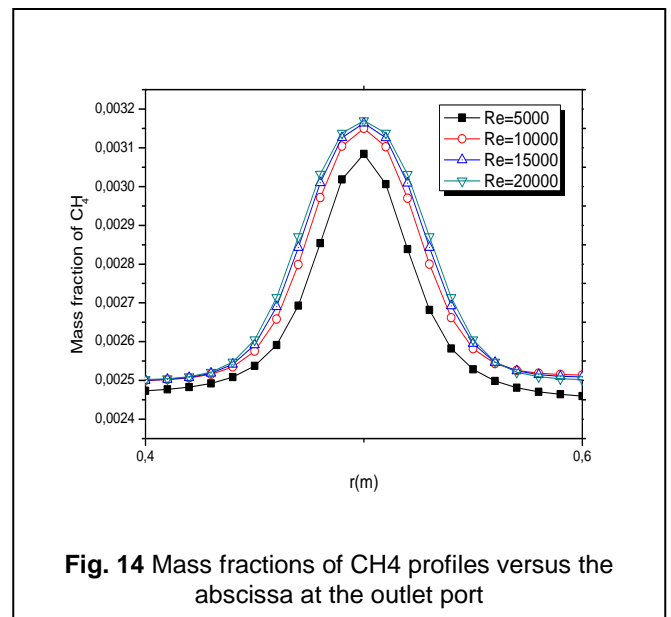
#### 4.3 Concentration fields

Fig.11 shows that, in the median plane, the iso-concentrations are similar to parabolas whose vertices are located on the symmetry axis of the incinerator. The mass fractions of the fume components decrease as the flow moves towards the exit. It can be noted that the concentrations fields of chemical species as  $C_2H_4$ ,  $CO$ ,  $H_2$ ,  $C$  and  $O_2$  not illustrated in this paper are similar to

the concentration field of  $CH_4$ . The minimum values of mass fractions are observed at the vicinity of the main flow zone characterized by parallel streamlines showing that combustion of smoke pollutant components takes place in the region located between the vertical walls and the main flow zone. This result is in agreement with the high values of isotherms observed in that zone (Fig. 7).



The effect of the Reynolds number on the concentrations distributions is illustrated in Fig. 11 and 12 for a duration  $t = 30s$  of combustion of smoke components. The iso-concentrations distributions are not affected significantly by the increase of the Reynolds number but the values of mass fractions increases with the Reynolds number due to the reduction of the residence time of smoke components in the incinerator. The effect of radiative transfers on the iso-concentrations distributions is investigated. It can be observed that the iso-concentrations patterns are not affected significantly by the radiative heat transfers (Fig. 13).



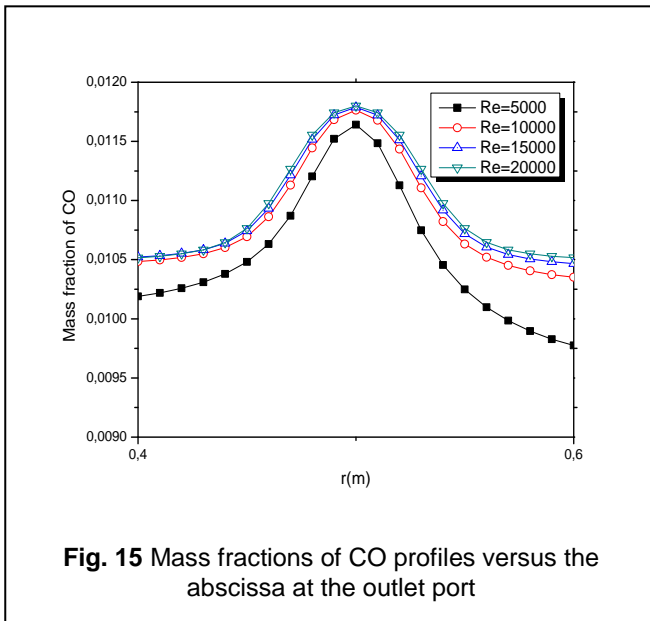


**Fig. 15** Mass fractions of CO profiles versus the abscissa at the outlet port

#### 4.4 The efficiency of thermo-destruction

The analysis of the evolution of smoke components mass fractions versus the abscissa in the vicinity of the exit of the incinerator shows that the thermo destruction of these components is not completely carried out (Fig. 14 and 15). The mass fractions of smokes component are maximum at the symmetry axis and decreases when the distance to this axis increases due to the fact that the combustion of smokes components takes place mainly in the zone located between the vertical walls and the main flow characterized by parallel streamlines. The smokes components are less destroyed when the Reynolds number is great due to the reduction of the residence time of smoke components.

#### 5 CONCLUSION

This paper presents numerical studies on the thermal treatment of the fumes produced by the combustion of municipal waste. The model is based on turbulent forced convection equations associated to the radiative transfer equation and to a one step-global chemical kinetics. Transfers equations are discretized using an implicit scheme based on the finite volume method. The algebraic equations obtained are solved using Gauss Seidel iterative method. Some of the important findings of the paper are:

- The results show that the pollutant components of the smoke are partially destroyed.
- The amount of heat released by the combustion of the pollutant components intensifies transfers but modifies weakly the flow structure.
- The radiative heat transfer has no effect on the flow structure but leads to an increase of the streamline values. The isotherms fields are weakly modified by the radiative transfer.
- The increasing values of the Reynolds number result in decreasing of the thermo destruction efficiency of the pollutant components of the smoke
- The thermo destruction process contribute to the reduction of the quantities of pollutants released by household waste incinerator

#### ACKNOWLEDGMENTS

The authors would like to thank the Co-operation Service and Cultural Activities of France Embassy in Togo for the financial support for the ongoing research on thermo destruction of household incineration flue gases.

#### NOMENCLATURE

$C_p$	specific heat of the fluid, ( $\text{Jkg}^{-1} \text{K}^{-1}$ )
$d_{in}$	inlet port size, (m)
$d_{out}$	outlet port size, (m)
$D$	furnace diameter, (m)
$D_k$	coefficient of diffusion, ( $\text{m}^2\text{s}^{-1}$ )
$G$	gravitational acceleration, ( $\text{m s}^{-2}$ )
$H$	furnace height, (m)
$hair$	heat transfer coefficient by natural convection, ( $\text{Wm}^{-2}\text{K}^{-1}$ )
$I$	radiative intensity, ( $\text{Wm}^{-2} \text{sr}^{-1}$ )
$K$	turbulent kinetic energy, ( $\text{m}^2\text{s}^{-2}$ )
$P$	pressure, (Pa)
$q_r$	radial radiative heat flux, ( $\text{Wm}^{-2}$ )
$Q_r$	dimensionless radial radiative heat flux, ( $Q_r = \pi q_r / n^2 \sigma T_0^4$ )
$R$	radial coordinate, (m)
$\vec{S}, \vec{S}'$	outward and inward radiation directions
$R_k$	Volumetric mass rate of species $i$ , ( $\text{kgm}^{-3} \text{s}^{-1}$ )
$R_t$	thermal resistance, ( $\text{KW}^{-1}$ )
$S_R$	volumetric radiative heat rate, ( $\text{Wm}^{-3}$ )
$S_h$	volumetric heat rate due to chemical reactions and radiation, ( $\text{Wm}^{-3}$ )
$T$	time, (s)
$T$	temperature, (K)
$Tu$	turbulent intensity, (%)
$U$	Axial velocity, ( $\text{m s}^{-1}$ )
$V$	radial velocity, ( $\text{m s}^{-1}$ )
$M_k$	molecular weight of species $k$ , ( $\text{kg mol}^{-1}$ )
$Y_k$	species mass fraction
$Z$	axial coordinate, (m)

#### Greek symbols

$B$	extinction coefficient, ( $\text{m}^{-1}$ )
$E$	turbulent kinetic energy dissipation rate, ( $\text{m}^2 \text{s}^{-3}$ )
$\sigma_k$	turbulent Prandtl number
$\sigma_\epsilon$	Schmidt number
$\Omega$	solid angle, (sr)
$\Phi$	scattering phase function
$\Lambda$	fluid thermal conductivity, ( $\text{W m}^{-1}\text{K}^{-1}$ )
$M$	Dynamic fluid viscosity, ( $\text{kg m}^{-1} \text{s}^{-1}$ )
$P$	fluid density, ( $\text{kgm}^{-3}$ )
$\kappa_a$	absorption coefficient, ( $\text{m}^{-1}$ )
$\sigma_s$	scattering coefficient, ( $\text{m}^{-1}$ )
$\gamma, \eta, \xi$	direction cosines

#### Subscripts

amb	ambient
E	effective
B	blackbody
in	inlet quantity
out	outlet quantity
t	turbulent
w	Wall



## REFERENCES

- Werkstoff 50, Springer-Verlag, pp. 479-484, 1992
- [1] B. K. Kho , K. G. Ashwani, "Brown gas incinerator for waste destruction and environmental pollution compliance," APEC Youth Scientist Journal, Vol. 4 / No.1, pp. 94-107
- [2] USEPA, "Recovery and Source Reduction," Report to the US Congress-Resource, USEPA Report SW-118, February 1978
- [3] C.R. Brunner, "Hazardous Waste Incineration", 2nd Edition, McGraw-Hill, New York, 1994
- [4] Gordon McKay, "Dioxin characterisation, formation and minimisation during municipal solid waste (MSW) incineration", Chemical Engineering Journal , vol. 86, pp. 343-368, 2002
- [5] C.Y. C. Chris , W. K. Donald , "Behaviour of metals under the conditions of roasting MSW incinerator fly ash with chlorinating agents," Journal of Hazardous Materials , Vol. 64, Issue 1, pp. 75–89, 1 January 1999
- [6] M. Nielsen, J. B. Illerup, C. L. Fogh, L. P. Johansen, "PM Emission from CHP Plants < 25MWe", DOC, National Environmental Research Institute of Denmark
- [7] M.B. Chang, C.H. Jen, H.T Wu, H.Y Lin, "Investigation on the emission factors and removal efficiencies of heavy metals from MSW incinerators in Taiwan," Waste Management & Research , vol. 21, pp. 218–224, 2003
- [8] D.B. Lukyanov, G. Sill, J.L. Ditre, W.K. Hall, "Comparison of Catalyzed and Homogeneous Reactions of Hydrocarbons for Selective Catalytic Reduction (SCR) of NO<sub>x</sub>," Journal of Catalysis , Vol. 153, Issue 2, pp. 265–274, May 1995
- [9] D.B. Lukyanov, G. Sill, J.L. Ditre, W.K. Hall, "Comparison of Catalyzed and Homogeneous Reactions of Hydrocarbons for Selective Catalytic Reduction (SCR) of NO<sub>x</sub>," Journal of Catalysis, Vol. 153, Issue 2, pp. 265–274, May 1995
- [10] W. B. Sang , A. R. Seon , D. K. Sang , "NO removal by reducing agents and additives in the selective non-catalytic reduction (SNCR) process,". Journal of Chemosphere, Vol. 65, Issue 1, pp.170–175, September 2006
- [11] M. Tayyeb Javed, Naseem Irfan, B.M. Gibbs, "Control of combustion-generated nitrogen oxides by selective non-catalytic reduction,". Journal of Environmental Management, Vol. 83, Issue 3, Pages 251–289, May 2007
- [12] C. Mezerette, P.Girard, A.M. Vergnet, " Environmental Aspects of Biomass Pyrolysis," Wood Forest Tropics, vol. 232, pp. 67–80, 1992 (in French)
- [13] D.Briane, J.Doat, A.Riedacker, " Technical Guide of the Carbonization Aix-en Provence, EDISUD (the Charcoal Production)," EDISUD, 1985 (in French)
- [14] P.Girard, "Analytical performance tests for charcoal-making technics and equipment," Holzals Rohund
- [15] K.Halouani, H.Farhat, "Depollution of atmospheric emissions of wood pyrolysis fumaces," Renewable energy A., vol. 28, n°1, pp. 129-138, 2003
- [16] K. N'Wuitcha, M. Banna, S.W. Igo, B. Zeghmati, K. Palm, X. Chesneau, "Numerical analysis of depollution of smoke produced by household wastes incineration," Journal of Heat transfer, vol. 134, pp. 041203-1, 041203-11, 2012
- [17] B.E. Launder, D.B. Spalding, "The numerical computation of turbulent flows," Comp. Meth. Appl. Mech. Eng. , vol.3, pp. 269 – 283, 1974
- [18] B.F. Magnussen, B.H. Hjertager, "On the mathematical modeling of turbulent combustion with special emphasis on soot formation and combustion," in: Proceedings of the Sixteenth Symposium (Int.) on Combustion, The Combustion Institute, Pittsburgh, pp. 719 – 730, 1976
- [19] Y.K. Man, "Assessment of axisymmetric radiative heat transfer in a cylindrical enclosure with the finite volume method," International Journal of Heat and Mass Transfer, Vol. 51, pp. 5144 – 5153, 2008
- [20] M. Miyamoto, Y. Katoh, J. Kurima, H. Saki, " Turbulent free convection heat transfer from vertical parallel plates," In Heat Transfer, eds C. L. Tien, V. P. Carey and J. K Ferrell, Vol.4. Hemisphere, Washington, DC, pp. 1593-1598, 1986